



**HAL**  
open science

## Elucidating venlafaxine metabolism in the Mediterranean mussel (*Mytilus galloprovincialis*) through combined targeted and non-targeted approaches

N. Ariza-Castro, Frédérique Courant, Thibaut Dumas, B. Marion, H. Fenet, Elena Gomez

### ► To cite this version:

N. Ariza-Castro, Frédérique Courant, Thibaut Dumas, B. Marion, H. Fenet, et al.. Elucidating venlafaxine metabolism in the Mediterranean mussel (*Mytilus galloprovincialis*) through combined targeted and non-targeted approaches. *Science of the Total Environment*, 2021, 779, pp.146387. 10.1016/j.scitotenv.2021.146387 . hal-03228661

**HAL Id: hal-03228661**

**<https://hal.science/hal-03228661>**

Submitted on 24 Apr 2023

**HAL** is a multi-disciplinary open access archive for the deposit and dissemination of scientific research documents, whether they are published or not. The documents may come from teaching and research institutions in France or abroad, or from public or private research centers.

L'archive ouverte pluridisciplinaire **HAL**, est destinée au dépôt et à la diffusion de documents scientifiques de niveau recherche, publiés ou non, émanant des établissements d'enseignement et de recherche français ou étrangers, des laboratoires publics ou privés.



Distributed under a Creative Commons Attribution - NonCommercial 4.0 International License

1 **Title**

2 Elucidating Venlafaxine Metabolism in the Mediterranean Mussel (*Mytilus*  
3 *galloprovincialis*) through Combined Targeted and Non-Targeted Approaches

4

5 N. Ariza-Castro<sup>1,3\*</sup>, F. Courant<sup>1</sup>, T. Dumas<sup>1</sup>, B. Marion<sup>2</sup>, H. Fenet<sup>1</sup> and E. Gomez<sup>1</sup>

6 <sup>1</sup>HydroSciences, IRD, CNRS, Université de Montpellier, Montpellier - \*nariza@itcr.ac.cr

7 <sup>2</sup>Institut des Biomolécules Max Mousseron, ENSCM, CNRS, Université de Montpellier, Montpellier, France

8 <sup>3</sup>Escuela de Química, Instituto Tecnológico de Costa Rica, Cartago 159-7050, Costa Rica

9

10

11 **Abstract**

12

13 Exposure of aquatic organisms to antidepressants is currently well documented, while little information is  
14 available on how wild organisms cope with exposure to these pharmaceutical products. Studies on  
15 antidepressant metabolism in exposed organisms could generate information on their detoxification  
16 pathways and pharmacokinetics. The goal of this study was to enhance knowledge on the metabolism of  
17 venlafaxine (VEN)—an antidepressant frequently found in aquatic ecosystems—in *Mytilus galloprovincialis*,  
18 a bivalve that is present worldwide. An original tissue extraction technique based on the cationic properties  
19 of VEN was developed for further analysis of VEN and its metabolites using targeted and non-targeted  
20 approaches. This extraction method was assessed in terms of recovery and matrix effects for VEN  
21 metabolites. Commercial analytical standards were applied to characterize metabolites found in mussels  
22 exposed to 10 µg/L VEN for 3 and 7 days. Targeted and non-targeted approaches using liquid  
23 chromatography (LC) combined with high-resolution mass spectrometry (HRMS) were implemented to  
24 screen for expected metabolites based on the literature on aquatic species, and for metabolites not  
25 previously documented. Four venlafaxine metabolites were identified, namely N-desmethylvenlafaxine and  
26 O-desmethylvenlafaxine, which were clearly identified using analytical standards, and two other metabolites  
27 revealed by non-target analysis. According to the signal intensity, hydroxy-venlafaxine (OH-VEN) was the  
28 predominant metabolite detected in mussels exposed for 3 and 7 days.

29

## 30 **Keywords**

31 Bioaccumulation, pharmaceuticals, metabolites, mass spectrometry, bivalves

32

## 33 **Highlights**

34 • An extraction method based on the cationic properties of VEN was successfully developed.

35 • The non-targeted approach allowed the identification of new VEN metabolites in mussels.

36

37 • OH-VEN was the predominant metabolite detected in VEN-exposed mussels.

38

## 39 **1 Introduction**

40 Venlafaxine (VEN), an antidepressant prescribed for the treatment of human clinical and anxiety  
41 disorders, is one of the most commonly detected pharmaceutically active compounds (PhACs) in the  
42 aquatic environment (Brieudes et al., 2017; Moreno-González et al., 2016; Paíga et al., 2019). This  
43 contamination affects the coastal marine environment, where recent studies have revealed the  
44 bioaccumulation of VEN, among other PhACs, in different species (Alvarez-Muñoz et al., 2015a,b;  
45 McEneff et al., 2013). Particularly, bivalves have shown the highest VEN accumulation (up to 36.0  
46 ng/g dw) in relation to other aquatic organisms such as microalgae and fish (Alvarez-Muñoz et al.,  
47 2015b). The Mediterranean mussel (*Mytilus galloprovincialis*) is a species commonly used in  
48 monitoring environmental contaminants in the marine environment thanks to its wide geographical  
49 distribution, its filter-feeding behavior and ability to bioaccumulate contaminants (Gomez et al., 2012;  
50 Silva et al., 2016)—it has also recently been used for assessing VEN metabolism. In laboratory VEN-  
51 exposed Mediterranean mussels, Serra-Compte et al. (2018) detected three phase I metabolites, i.e.  
52 O-desmethyl venlafaxine (ODV), N-desmethyl venlafaxine (NDV) and N,O-didesmethyl venlafaxine  
53 (NODDV), while Gomez et al. (submitted) detected four phase I metabolites, i.e. ODV, NDV, NODDV  
54 and N,N-didesmethyl venlafaxine (NNDDV). The two previous studies were conducted on the basis of  
55 a targeted analysis geared towards monitoring known phase I metabolites, already reported in the  
56 literature focused in humans. However, non-targeted approaches are promising to achieve a more  
57 complete characterization of VEN metabolism, including previously unreported metabolites in  
58 Mediterranean mussels. Non-targeted approaches are based on the generation of chemical profiles in

59 exposed and non-exposed organisms. Their comparison allow the detection of appearing signals in  
60 exposed organisms, those signals corresponding to potential previously unreported metabolites. This  
61 strategy helps elucidate biotransformation pathways in mussels, as already demonstrated for  
62 diclofenac (Bonnefille et al., 2017). Meanwhile, Jeon et al. (2013) conducted the first experiment to  
63 screen for VEN metabolites in freshwater crustaceans with a non-targeted approach using LC-HMRS,  
64 and the findings suggested the involvement of biotransformation pathways. These authors  
65 documented the structures of five VEN metabolites: three dealkylation products (ODV, NDV and  
66 NODDV, confirmed with reference standards) and two hydroxylation products (both with tentatively  
67 identified structures). In this context, to our knowledge no studies have focused on the VEN  
68 metabolism in mussels using an untargeted approach, thereby highlighting the question as to whether  
69 known biotransformation processes in humans are maintained in invertebrates. The goal of the  
70 present study was therefore to investigate this strategy for identifying VEN metabolites (already known  
71 and non-documented ones) produced in Mediterranean mussels (*M. galloprovincialis*) after exposure.  
72 A tissue treatment method based on the cationic properties of VEN and its metabolites (known in  
73 humans) was developed to increase the probability of metabolite detection and it was assessed in  
74 terms of recovery and matrix effect.

## 75 **2 Materials and Methods**

### 76 **2.1 Chemicals and materials**

77 VEN ( $\geq 98.5\%$ ), venlafaxine-d6 (VEN-d6,  $> 98\%$ ) and O-demethylvenlafaxine-d6 (ODV-d6,  $> 99.9\%$ )  
78 were purchased from Sigma-Aldrich (Steinheim, Germany). N,N-didesmethyl- O-desmethyl  
79 venlafaxine (NNDDODV,  $\geq 98\%$ ), ODV-glucuronide (ODV-glucu,  $> 98\%$ ) and NODDV-glucuronide  
80 (NODDV-gluco,  $\geq 95\%$ ) were purchased from Santa Cruz Biotechnology (Santa Cruz, CA, USA), while  
81 ODV, NDV, NNDDV and NODDV were obtained at analytical grade (purity  $\geq 98\%$ ) from Toronto  
82 Research Chemicals Inc. (Toronto, ON, Canada). Stock standard solutions of individual compounds  
83 were prepared at 100 mg/L concentration in methanol. Subsequent stock standard dilutions were  
84 prepared with methanol. All standard solutions were stored at  $-20^{\circ}\text{C}$ .

85 Ultrapure water was generated by the Millipore Simplicity UV system (Bedford, MA, USA) with a  
86 specific resistance of 18.2 M $\Omega$ .cm at  $25^{\circ}\text{C}$ . Dichloromethane (DCM) as pesticide analytical grade  
87 solvent, ammonia (NH<sub>3</sub>, 28%) as ACS reagent grade solution and HPLC/MS-grade solvents  
88 (methanol-MeOH and acetonitrile - ACN) were purchased from Carlo Erba (Val de Reuil, France).

89 Formic acid (98% purity) was obtained from Fisher Labosi (Elancourt, France) and ammonium acetate  
90 ( $\geq 98\%$ ) was purchased from Sigma-Aldrich (Steinheim, Germany). Dispersive SPE tubes containing  
91 Z-Sep-Plus (500 mg/12 mL) was obtained from Supelco (Bellefonte, PA, USA). Oasis<sup>®</sup> MCX 6 cc (150  
92 mg, 30  $\mu\text{m}$ , 6 cc) cartridges, obtained from Waters Corporation (Mildford, USA), and a Visiprep<sup>™</sup> DL  
93 Solid Phase Extraction (SPE) Vacuum Manifold from Supelco (Bellefonte, USA) were used for solid  
94 phase extraction. All chromatographic solvents were filtered through a 0.22  $\mu\text{m}$  nylon membrane filter  
95 (Nylaflo<sup>™</sup>, Michigan, USA). Glass-fiber filters (0.7  $\mu\text{m}$  pore size) purchased from Whatman  
96 (Maidstone, UK) were used to filter seawater.

## 97 **2.2 Experimental design and sample preparation**

98 *M. galloprovincialis* mussels were purchased in February 2017 from Mediterranean mussel suppliers  
99 (Bouzigues, France) and immediately transported to the laboratory. After cleaning, the mussels were  
100 acclimatized in aerated ( $9.9 \pm 0.4$  mg/L) filtered natural seawater (salinity =  $35 \pm 3$  g/L, pH =  $8.2 \pm 0.1$   
101 units) for 7 days before the experiment. During the acclimation and exposure periods, the seawater  
102 was renewed every day (static renewal), the room temperature was regulated at  $15 \pm 2^\circ\text{C}$ , and the  
103 mussels were fed *Tetraselmis suecica* phytoplankton (Greensea, Mèze, France) at constant density  
104 (10,000 cells/mL). 100 mussels (shell length 6.0–7.2 cm) were randomly distributed in 20 glass  
105 aquaria at a density of 5 mussels per 2 L water. Two groups were constituted: a solvent control group  
106 (with the vehicle for VEN: MeOH) and a group exposed at a nominal VEN concentration of 10  $\mu\text{g/L}$ .  
107 Each group consisted of 10 aquaria of 5 mussels each. During the exposure period, the VEN  
108 concentration was reestablished after daily water renewal. Seawater samples were taken daily to  
109 quantify VEN and its known metabolites. Mussels were sampled at days 3 and 7 of exposure (five  
110 aquaria per condition). All mussels were dissected and the digestive gland was frozen at  $-80^\circ\text{C}$  for  
111 further analysis, and the remaining soft tissues (the tissue of interest in our study) were frozen at  
112  $-80^\circ\text{C}$  before freeze-drying (Heto Power dry LL 3000, Thermo). After lyophilisation, these tissues were  
113 homogenized and ground into powder using an MM-2 vibrational mill (Retsch, Haan, Germany). Each  
114 sample was then placed inside a clean glass bottle and stored at room temperature in the dark until  
115 extraction and analysis. The mussel soft tissue analysis involved five replicates per group (solvent  
116 control and exposed) for each day of exposure (3 and 7 days).

## 117 **2.3 Sample extraction and LC-MS analysis**

### 118 **2.3.1 Tissue extraction method**

119 In order to increase the probability of detection of phase I and phase II (known and unknown) VEN  
120 metabolites in mussels, a tissue treatment method was developed using the physicochemical  
121 properties of these compounds, especially the positive charge on the amine functional group. 500 mg  
122 ( $\pm 1$  mg) dry weight (dw) of tissue samples obtained by pooling two individuals was weighed in a 50  
123 mL polypropylene centrifuge tube and spiked with VEN-d6 (500  $\mu\text{g}/\text{kg}$ ) and ODV-d6 (20  $\mu\text{g}/\text{kg}$ ). The  
124 tissues were then extracted by sonication in 5 mL of extraction solvent (5% formic acid in MeOH) for 5  
125 min. The samples were centrifuged at 23°C (3400 x g, 5 min) and the supernatant was decanted in  
126 another 50 mL polypropylene centrifuge tube. Re-extraction was carried out for each sample and the  
127 resulting supernatants were combined, and then 0.5 g of lipid removal sorbent Z-Sep Plus and 5 mL of  
128 5 mM ammonium acetate were added to the combined supernatant. The sample was then vortexed  
129 for 5 min and centrifuged at 23°C (3400 x g, 5 min). The extract obtained was transferred to a glass  
130 bottle (250 mL capacity) and diluted with milliQ water to a 150 mL final volume. After dilution, the  
131 sample pH was adjusted to  $1.4 \pm 0.1$ . Then water-diluted samples were loaded onto the SPE Oasis  
132 MCX cartridges pre-conditioned with MeOH (6 mL), milliQ water (6 mL) and 2% formic acid in water (6  
133 mL, pH: 1.40), respectively. After all samples were loaded at a flow rate of 1 mL/min, the cartridges  
134 were dried (until there were no longer any drops coming out of them) and then washed with 2% formic  
135 acid in water (6 mL, pH: 1.40), MeOH (2 mL), DCM (6 mL) and MeOH (3 mL). The analytes were  
136 eluted with 6 mL of 5% ammonium hydroxide in MeOH (5:95, v/v), and the solvent was evaporated to  
137 dryness under a gentle  $\text{N}_2$  stream at 35°C. The residues were reconstituted with 200  $\mu\text{L}$  of ACN:water  
138 (10:90, v/v). Finally, the sample was centrifuged at  $13.4 \times 10^3$  rpm for 10 min to separate the residual  
139 lipids. The clear solution was transferred to a vial for LC-MS analysis.

#### 140 **2.3.2 Seawater extraction method**

141 A tailored version of the tissue extraction and cleaning method was applied to determine the real VEN  
142 concentration in the seawater sampled during the mussel exposure period. 18 mL of seawater was  
143 spiked with surrogate standard (VEN-d6 at 1  $\mu\text{g}/\text{L}$ ) and adjusted to pH  $1.4 \pm 0.1$ . Solid-phase extraction  
144 was conducted with the same method used for the tissues, except for the washing step which was  
145 performed without DCM (6 mL). The analyte was eluted with fresh prepared ammonium hydroxide in  
146 MeOH and the solvent was evaporated to dryness under an  $\text{N}_2$  stream. The residue was reconstituted  
147 in 200  $\mu\text{L}$  of ACN:water (10:90, v/v) and transferred to a vial for LC-MS analysis.

#### 148 **2.3.3 Liquid chromatography and mass spectrometry conditions**

149 Extracts were analyzed on an HPLC Accela 600 pump coupled to a Q-Orbitrap HRMS mass  
150 spectrometer (Thermo Fischer Scientific) equipped with a heated electrospray ionization probe (HESI)  
151 source for detection. Chromatographic separation involved a reverse phase PFPP analytical column  
152 (Discovery HS F5 100 mm x 2.1 mm; 3  $\mu$ m particle size). The chromatography assays involved a 10  
153  $\mu$ L injection volume, a 0.35 mL/min flow rate and a binary gradient of ACN (A) and water (B), both  
154 containing 0.1% formic acid, as follows: 10% A at 0 min, 50% A at 4-6 min, 60% A at 8-10 min, 70% A  
155 at 14-16 min, 80% A at 17-19 min, 10% A at 21 min and a stop time at 27 min. Over a 27 min run,  
156 data acquisition was performed simultaneously in positive and negative ionisation mode and the HESI  
157 parameters were as follows: 55 arbitrary units (AU) sheath gas; 10 AU auxiliary gas; 275°C capillary  
158 temperature; 200°C heater temperature, and the electrospray voltage was set at 4.0/-4 kV. The S-lens  
159 radio frequency (RF) level was set at 100 AU. Full scan data in polarity switching mode were acquired  
160 at a resolution of 35,000 full width at half maximum (FWHM) with an automatic gain control (AGC) of  
161  $10^6$  and 250 ms of the maximum ion injection time. Moreover, MS<sup>2</sup> was achieved using a mass  
162 inclusion list composed of the mass of the precursor ion of the compounds of interest. A 10 eV  
163 absolute collision energy and 17,500 FWHM resolution of were used. The m/z scan range was set  
164 between 50-750.

#### 165 **2.4 Non-targeted metabolite analysis strategy**

166 Chemical profiles from five SC samples and five exposed samples at a nominal VEN concentration of  
167 10  $\mu$ g/L were generated by LC-HRMS for each exposure day (3 and 7 days). The data processing and  
168 signal identification strategies were from Bonnefille et al. (2017). Briefly, the data obtained in positive  
169 and negative ionization mode were converted with the free MS Convert software package (from \*.raw  
170 to \*mzxml) and extracted using an XCMS script (open source) on the basis of the R software. The  
171 XCMS parameters were tailored to fit our data: m/z interval for peak picking of 0.01, signal-to-noise  
172 ratio threshold of 5, group band-width of 20, with a 0.4 minimum fraction. After data processing, a 2-  
173 dimensional table containing information on each peak was generated (Courant et al., 2014). The  
174 peaks detected only in the exposed samples (absent in the control samples) and found in all five  
175 replicates were considered as potential VEN metabolites. The resulting signals were confirmed on the  
176 basis of the fold change and extracted ion chromatogram. The fold change was calculated as the ratio  
177 of the mean signal intensity in exposed samples to the mean signal intensity in the control samples.  
178 Only signals with a fold change higher than 10 in negative or positive ionization mode were kept and  
179 further processed to determine the structures associated with the signals. Moreover, extracted ion

180 chromatograms (EIC) were checked manually for all potential signals associated with metabolites so  
181 as to confirm the absence of any signal in the controls. Peaks associated with the same molecule (e.g.  
182 isotopes and/or dimers) were identified by checking the retention times and shapes of peaks obtained  
183 in the chromatograms generated by the Xcalibur QualAnalytical Browser (Xcalibur 3.0, Thermo Fisher  
184 Scientific Inc.). The same software was used to determine the elemental composition of unknown  
185 metabolites and those with the best fits, along with C, H, N and O compositions that could be related  
186 to VEN, are reported in the present study. Chromatographic retention time prediction of unknown  
187 metabolites was conducted using the multiple linear regression model developed by Jeon et al.  
188 (2013). With this model, an equation was obtained by plotting the retention time versus the molecular  
189 weight (MW) and the distribution coefficient ( $\log D_{ow}$ ) of the parent compound and its known  
190 metabolites. The MW and  $\log D_{ow}$  values were generated by ACD/ChemSketch (version 12.01).

## 191 **2.5 Targeted metabolite analysis**

### 192 **2.5.1 LC-MS analysis**

193 In the targeted analysis, only data acquired in positive electrospray ionization mode were considered,  
194 as this was the most sensitive mode for the molecules included in this section of the study (VEN and  
195 its known metabolites). Each compound was confirmed on the basis of: (1) the retention time, and (2)  
196 the mass accuracy (max 5 ppm deviation) of protonated molecules  $[M+H]^+$  in full scan MS mode  
197 compared to values obtained for the analytical standards under the same analytical conditions.

### 198 **2.5.2 Quantification of VEN and its known human metabolites in tissues**

199 In order to quantify VEN and its known metabolites in mussel soft tissues, calibration curves were  
200 plotted for blank mussel tissues by adding a fixed amount of the internal standards: VEN-d6 (500  
201  $\mu\text{g}/\text{kg dw}$ ) and ODV-d6 (20  $\mu\text{g}/\text{kg dw}$ ) and increasing quantities of the target analytes from 0 to 3000  
202  $\mu\text{g}/\text{kg dw}$  for VEN, and from 0 to 80  $\mu\text{g}/\text{kg dw}$  for its known phase I (ODV, NDV, NNDDV, NODDV and  
203 NNDDODV) and phase II (ODV-glucu and NODDV-glucu) metabolites before extraction.

### 204 **2.5.3 VEN quantification in seawater**

205 In addition, a seawater calibration curve was plotted by adding a fixed amount of internal standard  
206 VEN-d6 (at  $1\mu\text{g}/\text{L}$ ) and increasing quantities (0–15  $\mu\text{g}/\text{L}$ ) of the targeted VEN analyte in blank  
207 seawater.

### 208 **2.5.3 Method performances**



209 The method performances of both matrices were evaluated by taking into account aspects such as the  
210 linearity, limit of detection (LOD) of the methods, absolute recovery, matrix effects and repeatability

---

### Tissues

211 per analyte. Linearity was estimated with blank tests and calibration curves in tissues (five levels) at  
212 the 250–3000 µg/kg dw concentration range for VEN and 5–80 µg/kg dw for its known metabolites,  
213 and in seawater (seven levels) at 0.1–15 µg/L concentration range for VEN. LODs of the tissues and  
214 water methods were determined as the concentration resulting in a signal-to-noise ratio of 3 for each  
215 analyte. Absolute recoveries were studied by comparison of the signal area of each analyte in blank  
216 samples spiked before and after the extraction/purification process, both injected under the same  
217 analytical conditions. Matrix effects were evaluated by comparison of the signal area of each analyte  
218 in blank samples spiked after extraction/purification with the signal area of each analyte measured in a  
219 pure standard injected under the same analytical conditions. Absolute recovery, matrix effects and  
220 repeatability of the methods were evaluated by spiking tissues with 20 µg/kg (dw) and seawater with  
221 1µg/L of all compounds in triplicate.

### 222 **2.6 VEN bioconcentration factor and the mann Whitney non-parametric statistical test**

223 An apparent bioconcentration factor (BCFa) was calculated for VEN as the ratio of the measured  
224 concentration in the tissues to the measured concentration in seawater. The mann Whitney non-  
225 parametric statistical test was performed to compare the data obtained at 3 days and 7 days.  
226 OriginPro 2018 statistical software was used for this test.

## 227 **3. Results**

### 228 **3.1 Analytical performance**

229 The method performances are shown in Table 1. Both tissue and water methods demonstrated good  
230 linearity ( $r^2 > 0.98$ ) in the concentration range defined in both matrices for the 8 compounds included in  
231 the study. Absolute recoveries of phase I metabolites were higher than 91% in the tissues. Phase II  
232 metabolites had a lower absolute recovery (approximately 50%) in this matrix. A medium matrix effect  
233 was observed in tissues for all evaluated analytes (suppression between 32% and 59%). The average  
234 variability for all analytes evaluated never exceeded 21% in both matrices. The sensitivity of the  
235 methods in terms of LOD ranged from <1.0 to 8.0 µg/kg dw in tissues and was 1 ng/L in seawater.

236

Analyte	Table 1 Physicochemical properties, retention time, linearity, absolute recovery, matrix effects, average repeatability and method LODs and LOQs observed for each molecule in LC-MS Q-Orbitrap.									$\sigma_{\text{Meth}}$ ( $\mu\text{g dw}$ )
<b>NODD-glucuf</b>	425.47274	426.2122	2,78; 10,24	-3.58	3.96	0.9923	50 $\pm$ 7	-48 $\pm$ 3	17	8.0
<b>ODV-glucuf</b>	439.49932	440.2279	2,78; 9,26	-3.65	4.21	0.9993	49 $\pm$ 19	-51 $\pm$ 8	16	8.0
<b>NNDDODV<sup>e</sup></b>	235.32204	236.1645	9,72; 10,38	-1.79	6.96	0.9832	96 $\pm$ 4	-59 $\pm$ 6	21	3.0
<b>NODDV<sup>e</sup></b>	249.34862	250.1801	9,83; 10,59	-1.29	7.91	0.9988	98 $\pm$ 6	-41 $\pm$ 9	4	2.0
<b>ODV<sup>e</sup></b>	263.3752	264.1958	9,23; 10,04	-1.36	8.02	0.9886	100 $\pm$ 5	-32 $\pm$ 8	5	5.0
<b>NNDDV<sup>e</sup></b>	249.34862	250.1801	9,85; 14,75	-1.06	11.64	0.9987	97 $\pm$ 6	-55 $\pm$ 8	17	0.5
<b>NDV<sup>e</sup></b>	263.3752	264.1958	10,44; 14,83	-0.55	12.08	0.9945	108 $\pm$ 12	-32 $\pm$ 12	9	1.5
<b>VEN</b>	277.40178	278.2114	9,26; 14,84	-0.62	14.23	0.9998	105 $\pm$ 7	-32 $\pm$ 11	4	0.5

#### Seawater

<b>VEN</b>	-	-	-	14.18	0.9992	105 $\pm$ 11	14 $\pm$ 3	18	1,0 ( $\mu\text{g/L}$ )
------------	---	---	---	-------	--------	--------------	------------	----	-------------------------

237

238

239

240 <sup>a,b,c,d</sup> values predicted with ACD/ChemSketch software; <sup>e</sup>phase I metabolite and <sup>f</sup>phase II metabolite.

### 241 3.2 VEN quantification

242 The VEN concentrations were measured in water to control mussel exposure in aquaria. The  
 243 exposure concentrations measured in the exposed aquaria ranged from 9.5 to 12.5  $\mu\text{g/L}$  (Table 2). No  
 244 signal of the parent compound (VEN) was detected in the control samples (SC) of both matrices  
 245 (seawater and tissues). Mean VEN concentrations in exposed mussel tissues were around 1.9 mg/kg  
 246 dw and 2.5 mg/kg dw at days 3 and 7, respectively. Moreover, when considering the VEN  
 247 concentration measured in water and exposed mussel tissues, the apparent bioconcentration factors  
 248 (BCFa) were  $177 \pm 27$  L/kg dw and  $229 \pm 29$  L/kg dw for days 3 and 7, respectively. Finally, with the  
 249 Mann Whitney non-parametric statistical test, for VEN and its metabolites ODV and NDV, no  
 250 significant differences in the concentrations were observed between day 3 and day 7.

251

252

253

254

255

256

257

258 **Table 2** Mean concentrations of VEN and its metabolites NDV and ODV measured in the different conditions and  
 259 matrices (seawater and tissue) of the study.

Matrix	Conditions	Analytes		
		VEN ( $\mu\text{g/L}$ in water ou $\mu\text{g/kg}$ dw in tissue) (n=5)	NDV ( $\mu\text{g/L}$ in water ou $\mu\text{g/kg}$ dw in tissue) (n=5)	ODV ( $\mu\text{g/L}$ in water ou $\mu\text{g/kg}$ dw in tissue) (n=5)
Seawater	SC	< LOD	< LOD	< LOD
	Exposure	$11.0 \pm 1.5$	< LOD	< LOD
	SC	< LOD	< LOD	< LOD
Tissues	3rd day of exposure	$1948 \pm 493$	$50 \pm 13$	$28 \pm 7$
	7th day of exposure	$2517 \pm 341$	$34 \pm 13$	$24 \pm 8$

260

261

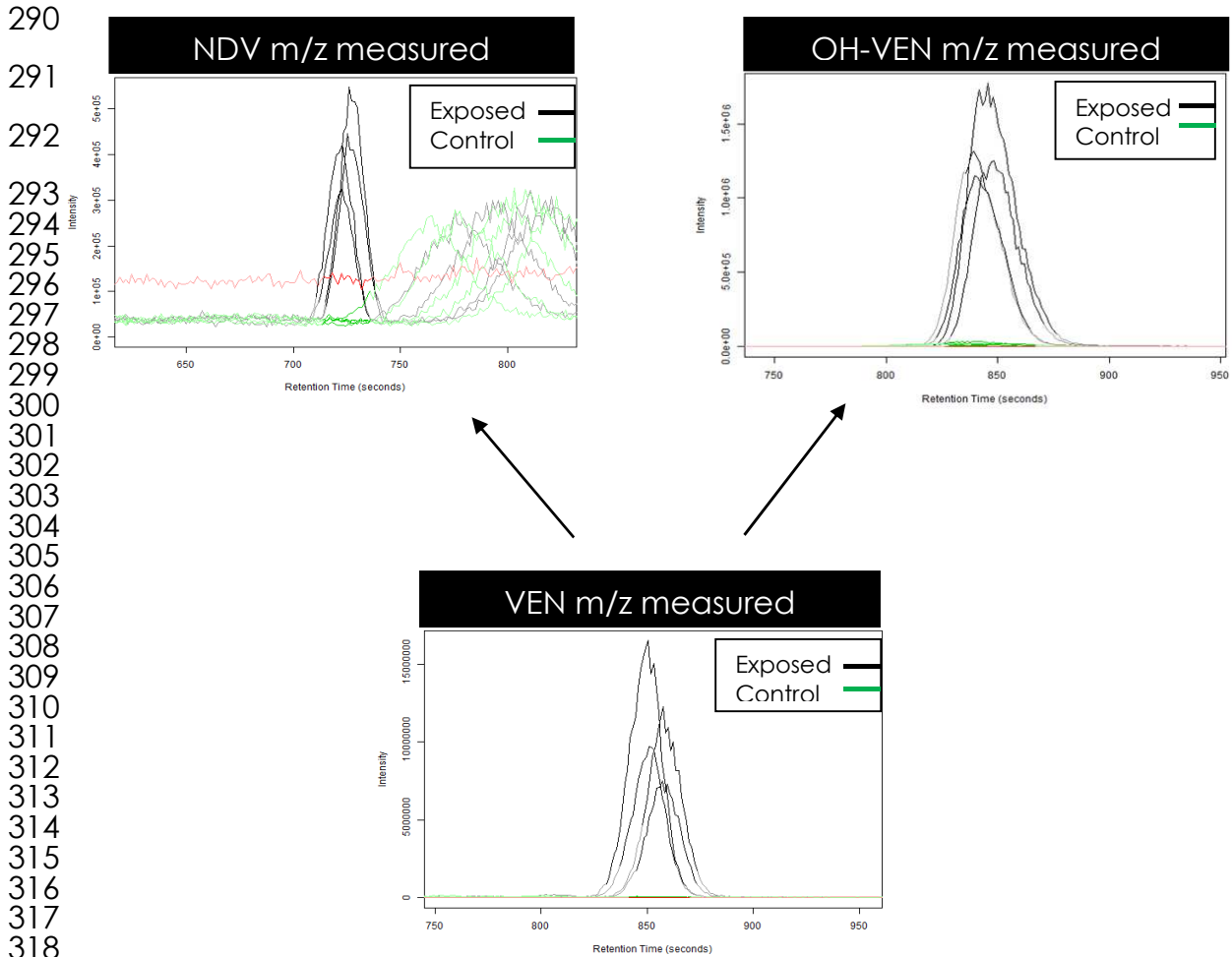
### 262 3.3 Non-targeted analysis of VEN and its metabolites in tissues

263 The non-targeted approach led to the detection of four metabolites. All of these molecules were  
 264 detected in positive mode, while no signal in the negative mode could be identified as a potential  
 265 metabolite. The metabolite and parent compound identification process is described below. Relevant  
 266 information on the identification of these molecules is also presented in Table 3.

#### 267 3.3.1 Venlafaxine

268 Among the signals detected in exposed mussels, absent in the control samples and found in all  
 269 replicates, a peak with molecular mass  $[\text{M}+\text{H}]^+$  278.2114 was identified at 14.23 min (i.e. M in Table  
 270 3). The selection of this signal was confirmed by its fold change value of 132 (value >10) and its  
 271 extracted ion chromatogram (Fig. 1). Xcalibur software helped determine the elemental composition of  
 272 the signal and the suggestion with the smallest delta atomic mass unit (amu) was considered. The  
 273 experimental mass  $[\text{M}+\text{H}]^+$  278.2114 associated with the retention time (14.23 min) and elemental  
 274 composition proposed ( $\text{C}_{17}\text{H}_{27}\text{NO}_2$ ) coincided with the identification of VEN (Table 1). The  
 275 experimental mass of VEN was compared with its theoretical mass and no difference was found  
 276 (Table 3). The identification of the signal corresponding to the isotopic ion  $^{13}\text{C}$  ( $[\text{M}+\text{H}]^+$  279.2148) at  
 277 14.26 min reconfirmed the presence of this molecule (VEN) (Fig. 2). HCD fragmentation (at 10 eV)  
 278 demonstrated the presence of a fragment at  $m/z$  260.2007 (Fig. 2, (1)). This fragment was associated  
 279 with the loss of 18.0107 amu compared to the measured VEN  $m/z$  278.2114, corresponding to a  
 280 neutral loss of  $\text{H}_2\text{O}$  in the VEN structure. In addition, the signal corresponding to the isotopic ion  $^{13}\text{C}$   
 281 ( $[\text{M}+\text{H}]^+$  261.2039) of this fragment was identified. A second fragment was observed at  $m/z$  215.1427  
 282 (Fig. 2, (2)). This fragment corresponded to a loss of 45.0580 amu (equivalent to a loss of  $\text{C}_2\text{H}_7\text{N}$ )

283 relative to the previously observed fragment in the VEN structure. A third fragment was found at m/z  
284 121.0646 (Fig. 2, (3)). The elemental composition of this fragment corresponded to C<sub>8</sub>H<sub>9</sub>O. Note that  
285 the signals corresponding to the fragments and <sup>13</sup>C isotopic ions had peak shapes and retention  
286 times very similar to those of VEN, thereby indicating that they were related. The VEN identification  
287 was confirmed by injection of the analytical standard under the same conditions reaching the  
288 maximum confidence level (level 1) in the identification of elucidated signals from a non-directed  
289 analysis, according to the scale proposed by Schymanski et al. (2014).



320 **Figure 1.** Examples of extracted ion chromatograms of metabolites (NDV and OH-VEN) and the parent compound  
 321 (VEN). Black peaks represent the exposed samples and green peaks are the control samples. No peaks were  
 322 identified in the control samples for these molecules.  
 323  
 324

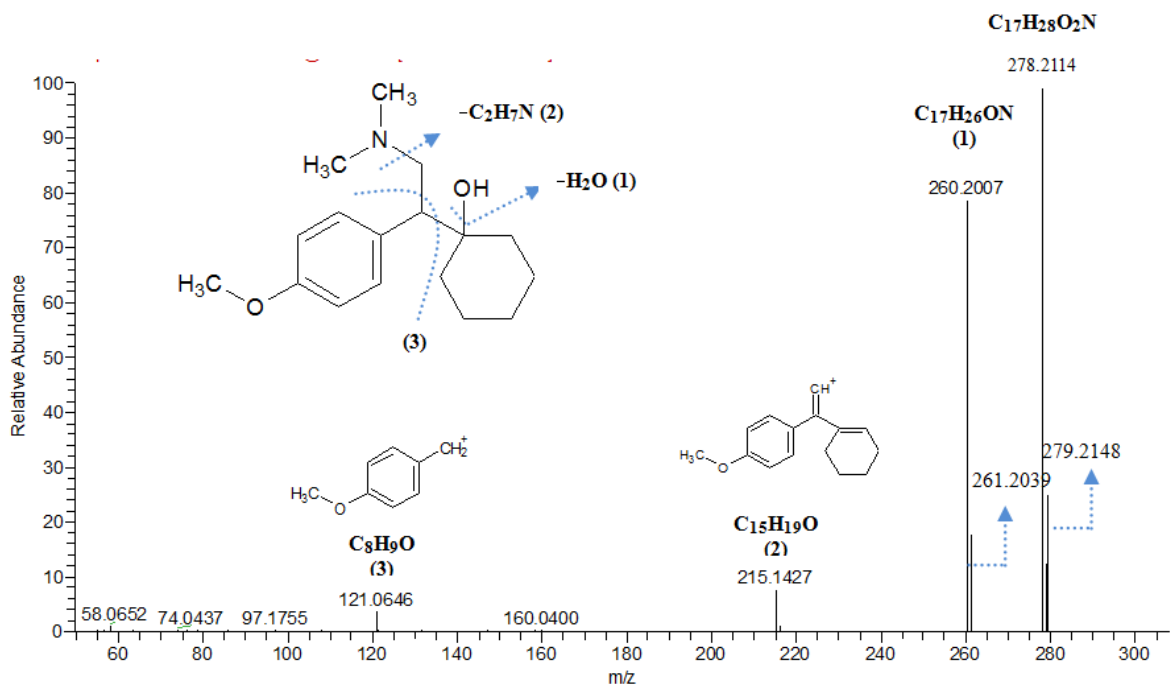


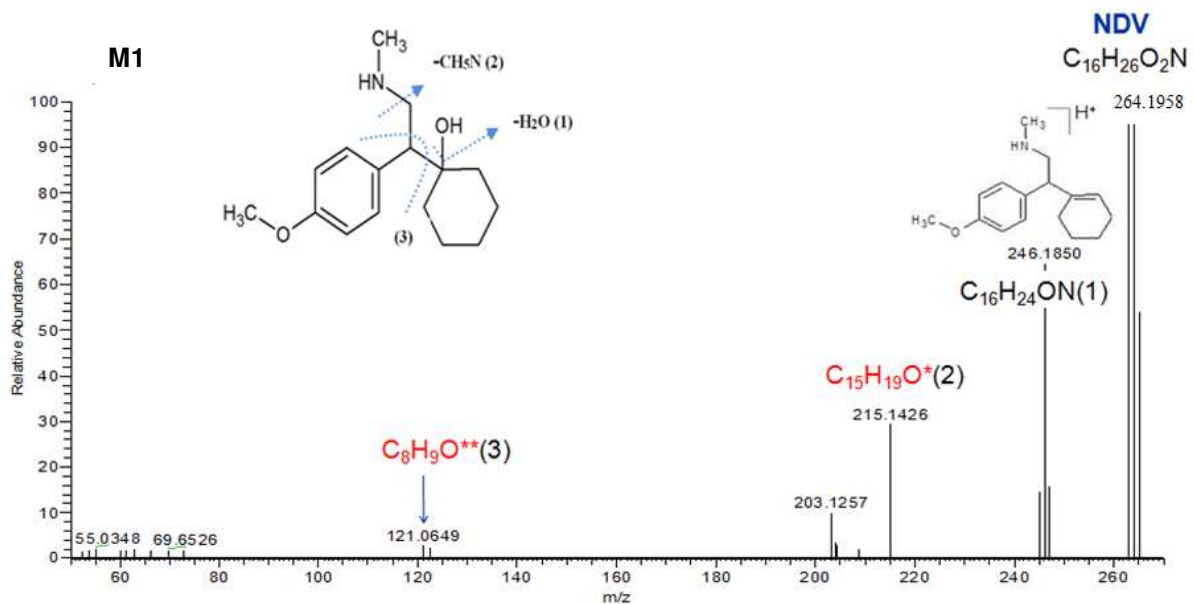
**Figure 2.** Relevant ions from the high resolution mass spectrum of fragmented VEN at 10 eV

328 **3.3.2 Phase I metabolites**

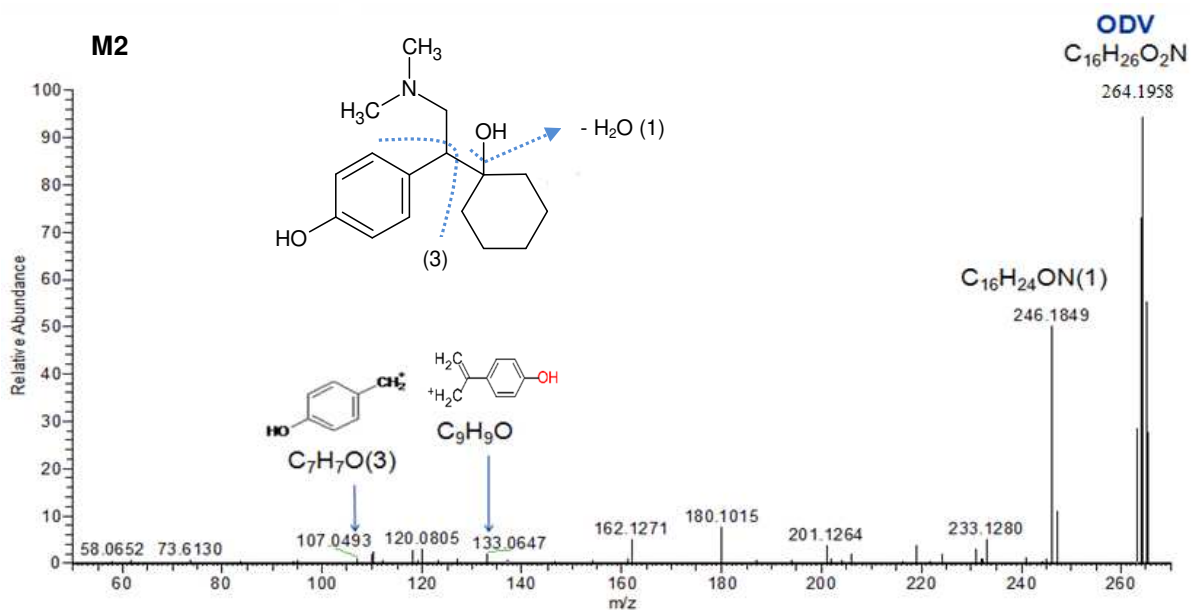
329 **3.3.2.1 Oxidative metabolism-demethylation**

330 Two metabolites identified as M1 and M2 (Table 3) displayed a  $[M+H]^+$  of 264.1958. The signals of  
331 both metabolites demonstrated a fold change higher than 10 and were detected only in the exposed  
332 samples (Fig. 1). They presented a mass decrease of 14.0156 amu (equivalent to a loss of  $CH_2$ )  
333 compared to the VEN structure, corresponding to dealkylation in the parent compound structure. M1  
334 and M2 exhibited different retention times, indicating that demethylation occurred at different positions.  
335 N-demethylation enabled greater interaction of nitrogen-free electron pairs with pentafluorophenyl  
336 propyl groups of the stationary phase in the chromatographic column used.

337



338



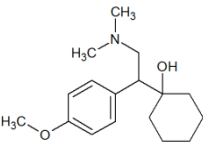
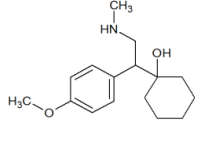
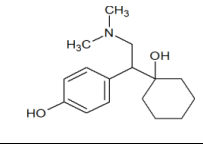
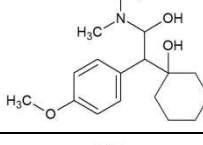
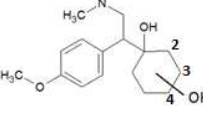
339

**Figure 3.** Relevant ions from the high resolution mass spectrum of fragmented NDV (**M1**) and ODV (**M2**) at 10 eV. Asterisks indicate fragments in common with the VEN fragmented spectrum.

340

**Table 3** Overview of VEN and its biotransformation products identified in mussel tissues by non-targeted analysis.

341

Peak ID	Tr (min)	Assignment	Elemental composition	Chemical Structure	Measured [M+H] <sup>+</sup> ( $\Delta m$ )	Fold change	Relevant [M+H] <sup>+</sup> fragment m/z, HCD 10 eV ( $\Delta m$ )	log D <sub>ow</sub> at pH 2 <sup>c</sup>	Tr predicted	$\Delta Tr$  observed-predicted <2	Confidence level
M	14.23	VEN	C <sub>17</sub> H <sub>27</sub> NO <sub>2</sub>		278.2114 (0.0 mmu)	132	260.2007 (0.7 mmu) 215.1427 (0.9 mmu) 121.0646 (0.7 mmu)	-0.62	13.15	1.08	Level 1
M1	12.08	NDV	C <sub>16</sub> H <sub>25</sub> NO <sub>2</sub>		264.1958 (0.0 mmu)	24	246.1850 (0.8 mmu) 215.1426 (1.0 mmu) 121.0649 (0.4 mmu)	-0.55	13.02	0.94	Level 1
M2	8.02	ODV	C <sub>16</sub> H <sub>25</sub> NO <sub>2</sub>		264.1958 (0.0 mmu)	43	246.1849 (0.9 mmu) 133.0647 (0.6 mmu) 107.0493 (0.4 mmu)	-1.36	9.20	1.18	Level 1
M3	14.11	OH-VEN	C <sub>17</sub> H <sub>27</sub> NO <sub>3</sub>		294.2064 (0.0 mmu)	1214	276.1952 (1.1 mmu) 233.1530 (1.1 mmu) 215.1425 (1.1 mmu) 178.1222 (1.0 mmu) 121.0644 (0.9 mmu)	-0.86	12.53	1.58	Level 2
M4	4.85	OH-VEN	C <sub>17</sub> H <sub>27</sub> NO <sub>3</sub>		294.2064 (0.0 mmu)	11	276.1955 (0.8 mmu) 121.0644 (0.9 mmu)	-2.05 (2) -2.06 (3) -1.98 (4)	6.93 (2) 6.88 (3) 7.26 (4)	2.1 (2) 2.0 (3) 2.4 (4)	Level 3

342

343

344 In these conditions, greater chromatographic retention was observed for the N-demethylated  
345 metabolite (M1;Tr: 12.08 min) compared to the O-demethylated metabolite (M2;Tr: 8.02 min) (Table  
346 3). For M1, three fragments were highlighted (Fig. 3), with the first one noted at m/z 246.1850,  
347 corresponding to H<sub>2</sub>O loss. The second one was detected at m/z 215.1426, corresponding to the  
348 elemental composition C<sub>15</sub>H<sub>19</sub>O. This fragment resulted from a CH<sub>5</sub>N loss consecutive to water loss,  
349 as observed with VEN but for a dealkylated metabolite, thus confirming N-dealkylation. The last  
350 fragment was detected at m/z 121.0649, corresponding to the elemental composition fragment C<sub>8</sub>H<sub>9</sub>O  
351 already observed for VEN (Fig. 3).

352 Concerning M2, a fragment was observed at m/z 246.1849 (equivalent to loss of H<sub>2</sub>O).  
353 HCD fragmentation demonstrated the presence of a second fragment at m/z 133.0647. With the  
354 assistance of Xcalibur software, the elemental composition proposed as the first option for this  
355 fragment was C<sub>9</sub>H<sub>9</sub>O (with a delta mm of -0.091) (Fig. 3) . Finally, a fragment was detected at m/z  
356 107.0493 and associated with the elemental composition fragment C<sub>7</sub>H<sub>7</sub>O, as observed with VEN but  
357 for a dealkylated metabolite. The presence of this fragment confirmed that a methyl group was  
358 detached from the oxygen of the VEN structure. The injection of analytical standards of NDV and ODV  
359 confirmed the identity of these metabolites at a confidence level of 1 in mussel tissues.

### 360 **3.3.2.1 Oxidative metabolism-hydroxylation**

361 Two metabolites, i.e. M3 and M4, revealed a [M+H]<sup>+</sup> of 294.2064. The M3 fold change value was  
362 higher than reported for M4, however both were greater than 10 (Table 3) and were detected only in  
363 the exposed samples (Fig. 1). The peak shapes and retention times of these signals (M3 and M4)  
364 differed from those observed for VEN, indicating that they were potential metabolites (Fig.1, Fig. 4 and  
365 Table 3). These metabolites presented a mass shift of +15.9950 compared to VEN. This mass shift  
366 could be associated with the biotransformation of an RH structure into an ROH structure, leading to  
367 the formation of potential hydroxylated metabolites. M3 and M4 exhibited shorter retention times than  
368 VEN, thus supporting the VEN hydroxylation hypothesis. Previous studies have highlighted the  
369 formation of such metabolites in organisms such as crustaceans (Jeon et al., 2013) and juvenile lean  
370 marine fish (Santos et al., 2020).

371

372

373



374  
375  
376  
377  
378  
379  
380  
381  
382  
383  
384  
385  
386  
387  
388  
389  
390  
391  
392  
393  
394  
395  
396  
397  
398  
399  
400  
401  
402  
403

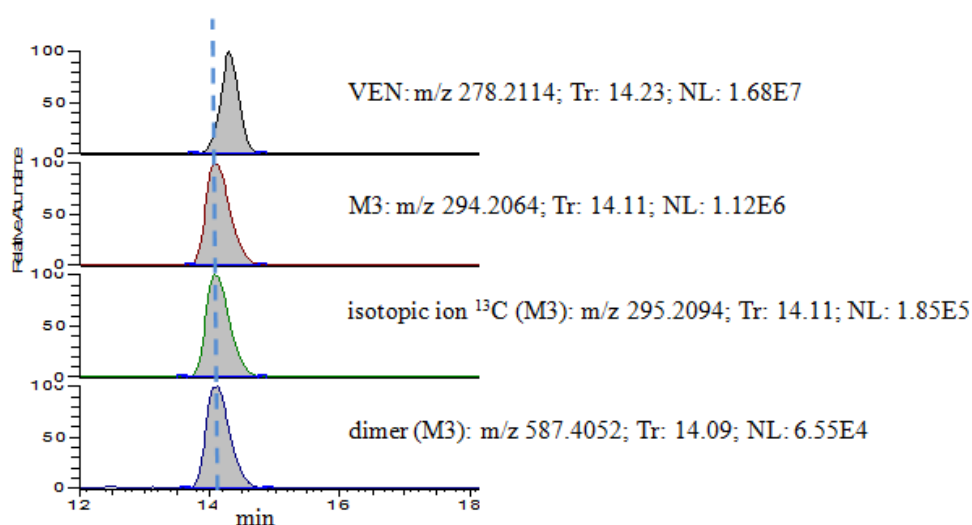
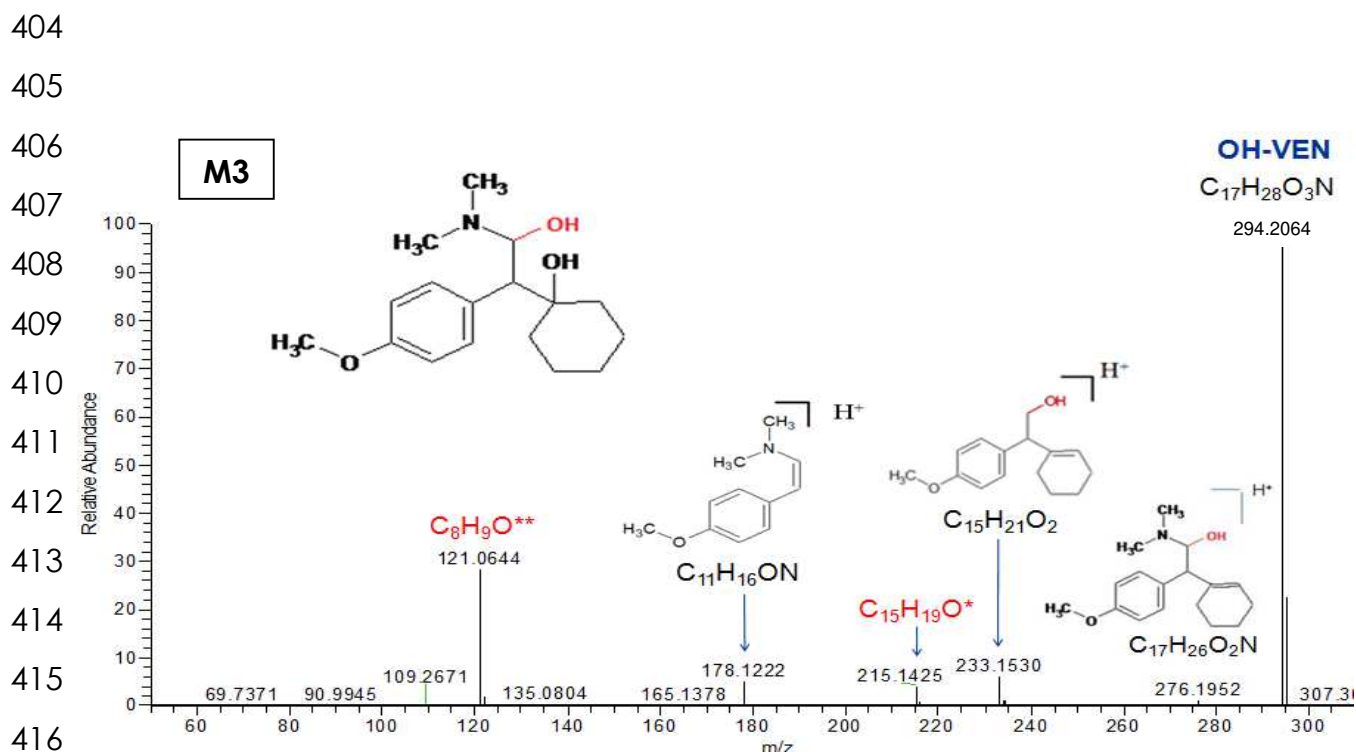


**Figure 4.** Chromatogram of signals associated with M3 ( $^{13}\text{C}$  isotopic ion and dimer). Comparison with VEN (Tr= retention time and NL=signal strength).

The addition of an OH group increases the molecular polarity, leading to earlier elution of the molecule in the reverse phase liquid chromatography system used. M3 showed a retention time of 14.11 min, while lower chromatographic retention was obtained for M4 (Tr: 4.85 min). The difference in retention times between M3 and M4 indicated that hydroxylation occurred at different positions in the parent compound (VEN).

For M3, two signals corresponding to (1) the  $^{13}\text{C}$  isotopic ion ( $[\text{M}+\text{H}]^+$  295.2094), and (2) the molecular dimer ( $[\text{M}+\text{H}]^+$  587.4052) observed at 14.11 min and 14.09 min, respectively, reconfirmed the presence of this potential metabolite (Fig. 4). HCD fragmentation of M3 showed a set of five fragments that allowed us to determine the position of the OH group in its structure (Fig. 5). The fragment at  $m/z$  276.1952 corresponded to  $\text{H}_2\text{O}$  loss from the initial molecule. The fragments observed at  $m/z$  215.1425 and 121.0644 in M1 were common to those of VEN. These coincidences between M3 and VEN fragments were evidence of the absence of OH group on the aromatic ring and on the hexane cycle of the initial molecule. The elementary compositions  $\text{C}_{15}\text{H}_{21}\text{O}_2$  and  $\text{C}_{11}\text{H}_{16}\text{ON}$  associated with fragments  $m/z$  233.1530 and 178.1222, respectively, confirmed the position of the OH group in the carbon adjacent to the VEN amino group.



417 **Figure 5.** Relevant ions from the high resolution mass spectrum of fragmented M3 at 10 eV. The  
418 asterisks indicate fragments in common with the VEN fragmented spectrum.

419  
420 In addition, in the absence of an analytical standard to ensure the identity of M3 at the maximum  
421 confidence level (level 1), a predictive chromatographic retention time model was applied to support  
422 our structure proposal for M3. This Tr prediction methodology was from Jeon et al. (2013). The  
423 chromatographic retention time was predicted using a multiple regression equation (Eq.1) formulated  
424 by plotting the retention time versus the molecular weight and the predicted log D<sub>ow</sub> of each compound  
425 with the available analytical standard (Table 1).

426 
$$\text{Retention time (Tr)} = 4.7107x \log D_{ow} + 0.0324x M \text{ (g/mol)} + 7.0762 \text{ (} r^2: 0.92 \text{)} \text{ (Eq.1)}$$

427 If the Tr predicted for the elucidated structure was within 2 min of the observed Tr, we considered that  
428 it was a viable structure. The proposed M3 structure demonstrated a predicted log D<sub>ow</sub> of -0.86 and a  
429 predicted Tr of 12.53 min, showing a difference of less than 2 min with respect to the observed Tr  
430 (Table 3). The proposed M3 structure was therefore feasible with a confidence level of 2.

431 The information available for M4 was limited. The signal intensity was very weak, which made it  
432 difficult to identify the relevant fragments. Only two fragments were identified. The experimental mass  
433 [M+H]<sup>+</sup> 276.1955 was associated with the H<sub>2</sub>O loss. A second fragment was observed at m/z

434 121.0644 and its elemental composition was  $C_8H_9O$ , as observed for VEN. The presence of this last  
435 fragment suggests that the additional OH group was not positioned in the aromatic ring. Three  
436 possible OH group positions were noted for M3 when applying the predictive chromatographic  
437 retention time model (Table 3). The M3 structure with the OH group at positions 2 and 3 of the hexane  
438 cycle showed predicted retention times at 6.93 min and 6.88 min, respectively (Table 3). Both  
439 positions had a delta retention time (calculated considering the observed and predicted value) of 2 min  
440 and might have fit a possible M4 structure. Due to the limited information available, the proposed M4  
441 structure had a confidence level of 3.

442

### 443 **3.4 Venlafaxine metabolite quantification**

444 The two phase I metabolites generated by demethylation of VEN previously highlighted in mussel  
445 tissues were quantified on each exposure day (days 3 and 7). Mean concentrations of NDV ( $50 \pm 13$   
446 and  $34 \pm 13 \mu\text{g}/\text{kg dw}$ ) and ODV ( $28 \pm 7$  and  $24 \pm 8 \mu\text{g}/\text{kg}$ ) were measured in tissues exposed to VEN  
447 for 3 and 7 days (Table 2). Considering the intensity obtained for hydroxylated M3 (i.e.  $1.5 \cdot 10^6$  versus  
448  $5 \cdot 10^5$  for M1), it seems (hypothesis put forward in the absence of absolute quantification) that it was  
449 the most abundant of all of the metabolites identified in this study. However, M3 quantification was not  
450 possible due to the lack of a commercially available analytical standard.

451

## 452 **4. Discussion**

453 PhACs for human care such as VEN are continuously disseminated in the environment (Čelić et al.,  
454 2019; Paíga et al., 2016, Santos et al., 2016), resulting in high exposure of non-targeted organisms to  
455 these pollutants, even at low concentrations. VEN has been demonstrated to bioaccumulate and  
456 interact at the molecular level with aquatic organisms, thereby impacting their tissue metabolic  
457 capacities and jeopardizing their adaptive response to an acute stressor, as noted by Best et al. (2014)  
458 and Ings et al. (2012). In addition, VEN has been shown to have an impact on the behavior (Malvault  
459 et al., 2018), reproduction (Parrott and Metcalfe, 2017) and survival (Schultz et al., 2011) of these  
460 organisms, but little information is available on the VEN metabolism process involved. In-depth  
461 knowledge on the metabolism of this substance in wildlife is necessary to unravel key events in the  
462 potential toxicological pathways. Metabolic studies in a broad range of organism are very challenging

463 but could benefit from advances in chemical analysis and combined targeted and non-targeted  
464 approaches, the latter recently used to elucidate small molecules such as metabolites (Bonefille et al.,  
465 2017; Santos et al., 2020). The present study in a marine invertebrate illustrates the potential offered  
466 by these non-targeted approaches for biomonitoring and conducting surveys on the marine  
467 environment.

468 The sample treatment step is crucial in the determination of unknown metabolites. The tissue  
469 treatment method was developed based on the physicochemical properties of known VEN metabolites  
470 in the human body (five phase I and two phase II metabolites). These compounds showed medium to  
471 high polarity, so the MeOH solvent was ideal for their extraction. VEN and its metabolites have a basic  
472 character due to the amine functional group present in their structures. A pH at least two units lower  
473 than the pKa value favors the presence of a positive charge on the nitrogen of the amine group of  
474 these compounds. Since the compounds of interest had this property, the sorbent SPE chosen  
475 combined two mechanisms to enhance their retention, i.e. strong cation exchange and hydrophobic  
476 interactions. This double retention mechanism enabled the recovery of phase I metabolites, but also of  
477 glucuronide metabolites, which are highly complex due to their elevated polarity and sensitivity to  
478 hydrolysis during the extraction process (Karinen et al., 2009; Ketola and Hakala, 2010). The  
479 analytical method performance evaluation showed that the combined tissue extraction and purification  
480 conditions enabled high absolute recoveries of phase I metabolites and glucuronide metabolites, along  
481 with moderate matrix effects.

482 Application of the tissue treatment method to the VEN-exposed samples generated data that helped  
483 determine the extent of parent compound accumulation in mussel tissues. The BCF values obtained  
484 ( $177 \pm 27$  L/kg dw and  $229 \pm 29$  L/kg dw for VEN exposure at days 3 and 7, respectively) were in a  
485 range similar to those already reported for VEN-exposed mussels. A first study conducted in mussels  
486 (*M. galloprovincialis*) exposed for 7 days to 1, 10 and 100  $\mu\text{g/L}$  VEN reported BCF values of  $178 \pm 8.0$   
487 L/kg dw,  $146 \pm 35$  L/kg dw and  $189 \pm 15$  L/kg dw, respectively (Gomez et al, submitted). In a second  
488 study, the BCF values reported for mussels (*M. galloprovincialis*) exposed for 20 days to  $10.7 \pm 1.6$   
489  $\mu\text{g/L}$  of VEN were between 213.3 and 528.1 L/kg dw for the different treatments applied while also  
490 taking the effects of water warming and acidification into account (Serra-Compte et al., 2018). The  
491 authors suggested that the positive ionized form of VEN would facilitate its adhesion to the biological  
492 matrix, which could explain the high BCF value obtained.

493 The high VEN bioconcentration combined with the presence of cytochrome P450 in mussels favours  
494 enzymatic reactions involved in the metabolism of this xenobiotic compound in mussels (Snyder,  
495 2000). The application of a non-targeted approach to samples collected in VEN-exposed mussels led  
496 to the identification of four phase I metabolites. Two metabolites resulted from the demethylation  
497 process at two different VEN positions: N-demethylation and O-demethylation. These metabolites  
498 have already been previously identified in laboratory-exposed mussels (Serra-Compte et al., 2018;  
499 Gomez et al., submitted) and in mussels collected in coastal areas of France (Martínez Bueno et al.,  
500 2014), Portugal, Italy and Spain (Álvarez-Muñoz et al., 2015b). Both metabolites presented  
501 concentrations two orders of magnitude lower than the parent molecule. This behavior may be  
502 expected in the mussel detoxification process, where it is sought to produce more hydrophilic and less  
503 toxic metabolites, thereby facilitating their excretion. Quantification of these metabolites showed that,  
504 for both exposure days, in the tested mussels there was a slight trend in favor of the detoxification  
505 pathway that generates VEN dealkylation at the nitrogen position, whereas ODV is the major  
506 metabolite in humans (Sanguhl et al., 2014). A similar behavior was observed by Santos et al.  
507 (2020), showing that N-demethylated metabolites are the predominant ones in fish. They suggest that  
508 due to the higher hydrophilic character of NDV at physiological pH compared to ODV, fish prefer to  
509 metabolize venlafaxine to NDV, generating higher concentrations of this metabolite in fish. The above  
510 explanation could potentially be the justification for the higher presence of NDV evidenced in mussels.  
511 Finally, NDV and ODV metabolites were both formed early during the detoxification process since they  
512 both presented higher concentrations at day 3. This was already observed in a previous study (Gomez  
513 et al., submitted). However, the findings of the non-parametric statistical Mann Whitney test comparing  
514 data obtained on days 3 and 7 revealed no significant differences between these days.

515 The two other metabolites identified were hydroxylated VEN metabolites at two different positions: 1)  
516 on the carbon adjacent to the amine group, and 2) on the hexane cycle. Hydroxylation is one of the  
517 two known N-dealkylation mechanisms. This mechanism involves formal hydroxylation of a C-H bond  
518 on the carbon adjacent to the heteroatom (HAT, H-atom transfer) (Meunier et al., 2004). The above  
519 findings support the hypothesis of the proposed structure for the VEN hydroxylated metabolite (M3),  
520 which to our knowledge has not been previously described. This metabolite showed the highest  
521 intensities of all metabolites identified in the study for both exposure days. Hydroxylated metabolites  
522 were also shown to be major diclofenac metabolites in mussels (Bonnefille et al., 2017; Świacka et al.,

523 2019). This also highlights the differences in biotransformation processes in mussels compared to  
524 humans (Sanguhl et al., 2014). Due to the low intensity of the second hydroxylated venlafaxine  
525 metabolite (M4), there was not a sufficient number of fragments to increase the confidence level for  
526 the suggested structure. This hydroxylated metabolite has been previously identified in crustaceans  
527 (Jeon et al., 2013). Both hydroxylated metabolites (M3 and M4) were formed later during the  
528 detoxification process since they both showed higher intensities at day 7.

529 No glucuronide metabolites were detected despite the fact that the method was found to be able to  
530 retain glucuronide metabolites. This could possibly be explained by two hypotheses: 1) mussels are  
531 not capable of producing glucuronides, or 2) the concentration at which these compounds are formed  
532 is below the detection limit of our method. A previous study revealed that mussels are capable of  
533 generating glucuronide metabolites from xenobiotic benzo(a)pyrene (Michel et al., 1995). Mussels  
534 may therefore possibly be able to generate this type of metabolite from pharmaceuticals. The above  
535 suggests that the concentration of these metabolites in the analyzed tissues was lower than our  
536 detection limit.

## 537 **5. Conclusions**

538 The non-targeted approach was demonstrated to be a relevant method for characterizing and  
539 identifying VEN metabolites produced in Mediterranean mussels, thereby generating insight into the  
540 VEN metabolism in mussels. Two hydroxylated metabolites were identified for the first time in this  
541 organism, thus confirming its ability to efficiently dealkylate and then hydroxylate amino  
542 pharmaceuticals. However, glucuronidation did not appear to be a major detoxification pathway for  
543 these compounds. Our results showed that mussels did not share the same VEN metabolism pathway  
544 as in humans, and N-demethylation appeared to be the main metabolization pathway in  
545 Mediterranean mussels. This hydroxylation ability thus facilitates further interpretation of metabolism in  
546 mussels. The identified metabolites could also be used as biomarkers of exposure to environmental  
547 pollutants. It should be noted that despite the active metabolism of mussels, venlafaxine  
548 bioaccumulates 117 times in this organism. This warrants further studies on the effects of these  
549 metabolites and venlafaxine in mussels.

## 550 **Acknowledgments**

551 The authors would like to thank the French National Research Agency (IMAP ANR-16-CE34-0006-01)  
552 and *Vicerrectoría de Investigación y Extensión del Instituto Tecnológico de Costa Rica* for funding. We  
553 also thank David Rosain and Céline Roques of the University of Montpellier for technical assistance in  
554 the laboratory and David Manley, English translator, for reviewing this document. The analyses were  
555 performed at the Platform Of Non-Target Environmental Metabolomics (PONTEM) member of the  
556 BioCampus Montpellier Alliance for Metabolomics and Metabolims Analysis (MAMMA) facility,  
557 Montpellier (France). This work benefitted from the French "Aquatic Ecotoxicology" framework which  
558 aims at fostering stimulating scientific discussions and collaborations in favor of more integrative  
559 approaches.

## 560 **References**

- 561 Alvarez-Muñoz, D., Huerta, B., Fernandez-Tejedor, M., Rodríguez-Mozaz, S., Barceló, D., 2015a.  
562 Multi-residue method for the analysis of pharmaceuticals and some of their metabolites in  
563 bivalves. *Talanta* 136, 174–182.
- 564 Álvarez-Muñoz, D., Rodríguez-Mozaz, S., Maulvault, A.L., Tediosi, A., Fernández-Tejedor, M., Van  
565 den Heuvel, F., Kotterman, M., Marques, A., Barceló, D., 2015b. Occurrence of pharmaceuticals  
566 and endocrine disrupting compounds in macroalgae, bivalves, and fish from coastal areas in  
567 Europe. *Environ. Res.* 143, 56–64.
- 568 Best, C., Melnyk-Lamont, N., Gesto, M., Vijayan, M.M., 2014. Environmental levels of the  
569 antidepressant venlafaxine impact the metabolic capacity of rainbow trout. *Aquat. Toxicol.* 155,  
570 190–198.
- 571 Bonnefille, B., Arpin-Pont, L., Gomez, E., Fenet, H., Courant, F., 2017. Metabolic profiling identification  
572 of metabolites formed in Mediterranean mussels (*Mytilus galloprovincialis*) after diclofenac  
573 exposure. *Sci. Total Environ.* 583, 257–268.
- 574 Briudes, V., Lardy-Fontan, S., Vaslin-Reimann, S., Budzinski, H., Lalere, B., 2017. Development of a  
575 multi-residue method for scrutinizing psychotropic compounds in natural waters. *J. Chromatogr.*  
576 *B Anal. Technol. Biomed. Life Sci.* 1047, 160–172.
- 577 Čelić, M., Gros, M., Farré, M., Barceló, D., Petrović, M., 2019. Pharmaceuticals as chemical markers  
578 of wastewater contamination in the vulnerable area of the Ebro Delta (Spain). *Sci. Total Environ.*  
579 652, 952–963.

580 Courant, F., Antignac, J.-P., Dervilly-Pinel, G., Le Bizec, B., 2014. Basics of mass spectrometry based  
581 metabolomics. *Proteomics* 14:2369–2388.

582 Gomez, E., Bachelot, M., Boillot, C., Dominique, M., Chiron, S., Casellas, C., Fenet, H., 2012.  
583 Bioconcentration of pharmaceuticals (benzodiazepines) and two personal care products (UV  
584 filters) in marine mussels (*Mytilus galloprovincialis*) under controlled laboratory  
585 conditions). *Environ. Sci. Pollut. Res.* 19:2561-2569.

586 Gomez, E., Boillot, C., Martinez Bueno, M.J., Munaron, D., Mathieu, O., Courant, F., Fenet, H. In vivo  
587 exposure of marine mussel to venlafaxine: bioconcentration and metabolization. Submitted

588 Ings, J.S., George, N., Peter, M.C.S., Servos, M.R., Vijayan, M.M. Venlafaxine and atenolol disrupt  
589 epinephrine-stimulated glucose production in rainbow trout hepatocytes. *Aquat. Toxicol.* 106-  
590 107, 48-55.

591 Jeon, J., Kurth, D., Hollender, J., 2013. Biotransformation pathways of biocides and pharmaceuticals  
592 in freshwater crustaceans based on structure elucidation of metabolites using high resolution  
593 mass spectrometry. *Chem. Res. Toxicol.* 26, 313–324.

594 Karinen, R., Andersen, J.M., Ripel, Å., Hasvold, I., Hopen, A.B., Mørland, J., Christophersen, A.S.,  
595 2009. Determination of heroin and its main metabolites in small sample volumes of whole blood  
596 and brain tissue by reversed-phase liquid chromatography-tandem mass spectrometry. *J. Anal.*  
597 *Toxicol.* 33, 345–350.

598 Ketola, R., Hakala, K., 2010. Direct analysis of glucuronides with liquid chromatography-mass  
599 spectrometric techniques and methods. *Curr. Drug Metab.* 11, 561–582.

600 Martínez Bueno, M.J., Boillot, C., Munaron, D., Fenet, H., Casellas, C., Gómez, E., 2014. Occurrence  
601 of venlafaxine residues and its metabolites in marine mussels at trace levels: Development of  
602 analytical method and a monitoring program. *Anal. Bioanal. Chem.* 406, 601–610.

603 Maulvault, A.L., Santos, L.H.M.L.M., Paula, J.R., Camacho, C., Pissarra, V., Fogaça, F., et al., 2018.  
604 Differential behavioural responses to venlafaxine exposure route, warming and acidification in  
605 juvenile fish (*Argyrosomus regius*). *Sci. Total Environ.* 634, 1136–1147

606 McEneff, G., Barron, L., Kelleher, B., Paull, B., Quinn, B., 2013. The determination of pharmaceutical  
607 residues in cooked and uncooked marine bivalves using pressurised liquid extraction, solid-



608 phase extraction and liquid chromatography-tandem mass spectrometry. Anal. Bioanal. Chem.  
609 405, 9509–9521.

610 Meunier, B., de Visser, S.P., Shaik, S., 2004. Mechanism of oxidation reactions catalyzed by  
611 cytochrome P450 enzymes. Chem. Rev. 104, 3947–3980.

612 Michel, X.R., Beasse, C., Narbonne, J., 1995. In vivo metabolism of benzo ( a ) pyrene in the mussel  
613 *Mytilus galloprovincialis*. Arch. Environ. Contam. Toxicol. 28, 215–222.

614 Moreno-González, R., Rodríguez-Mozaz, S., Huerta, B., Barceló, D., León, V.M., 2016. Do  
615 pharmaceuticals bioaccumulate in marine molluscs and fish from a coastal lagoon? Environ.  
616 Res. 146, 282–298.

617 Paíga, P., Santos, L.H.M.L.M., Ramos, S., Jorge, S., Silva, J.G., Delerue-Matos, C., 2016. Presence  
618 of pharmaceuticals in the Lis river (Portugal): sources, fate and seasonal variation. Sci. Total  
619 Environ. 573, 164–177.

620 Paíga, P., Correia, M., Fernandes, M., Silva, A., Carvalho, M., Vieira, J., Jorge, S., Silva, J., Freire, C.,  
621 Delerue-Matos, C., 2019. Assessment of 83 pharmaceuticals in WWTP influent and effluent  
622 samples by UHPLC-MS/MS : Hourly variation. Sci. Total Environ. 648, 582–600.

623 Parrott, J.L., Metcalfe, C.D., 2017. Assessing the effects of the antidepressant venlafaxine to fathead  
624 minnows exposed to environmentally relevant concentrations over a full life cycle. Environ.  
625 Pollut. 229, 403–411.

626 Sangkuhl, K., Stingl, J., Turpeinen, M., Altman, R., Klein, T., 2014. PharmaGKB summary: venlafaxine  
627 pathway. Pharmacogenet Genom. 24, 62–72.

628 Santos, L.H.M.L.M., Ramalhosa, M.J., Ferreira, M., Delerue-Matos, C., 2016. Development of a  
629 modified acetonitrile-based extraction procedure followed by ultra-high performance liquid  
630 chromatography–tandem mass spectrometry for the analysis of psychiatric drugs in sediments.  
631 J. Chromatogr. A 1437, 37–48.

632 Santos, L.H.M.L.M., Maulvault, A.L., Jaén-Gil, A., Marques, A., Barceló, D., Rodríguez-Mozaz, S.,  
633 2020. Insights on the metabolization of the antidepressant venlafazine by meagre (*Argyrosomus*  
634 *regius*) using a combined target and suspect screening approach. Sci. Total Environ. 737,  
635 140226

636 Schultz, M.M., Painter, M.M., Bartell, S.E., Logue, A., Furlong, E.T., Werner, S.L., et al., 2011.  
637 Selective uptake and biological consequences of environmentally relevant antidepressant  
638 pharmaceutical exposures on male fathead minnows. *Aquat. Toxicol.* 104, 38–47.

639 Schymanski, E.L., Jeon, J., Gulde, R., Fenner, K., Ru, M., Singer, H.P., Hollender, J., 2014. Identifying  
640 Small Molecules via High Resolution Mass Spectrometry: Communicating Confidence. *Environ.*  
641 *Sci. Technol.* 48, 2097–2098.

642 Serra-Compte, A., Maulvault, A.L., Camacho, C., Álvarez-Muñoz, D., Barceló, D., Rodríguez-Mozaz,  
643 S., Marques, A., 2018. Effects of water warming and acidification on bioconcentration,  
644 metabolism and depuration of pharmaceuticals and endocrine disrupting compounds in  
645 marine mussels (*Mytilus galloprovincialis*). *Environ. Pollut.* 236, 824–834.

646 Silva, L.J.G., Martins, M.C., Pereira, A.M.P.T., Meisel, L.M., Gonzalez-Rey, M., Bebianno, M.J., Lino,  
647 C.M., Pena, A., 2016. Uptake, accumulation and metabolism of the antidepressant fluoxetine  
648 by *Mytilus galloprovincialis*. *Environ. Pollut.* 213, 432–437.

649 Snyder, M.J., 2000. Cytochrome P450 enzymes in aquatic invertebrates: Recent advances and future  
650 directions. *Aquat. Toxicol.* 48, 529–547.

651 Świacka, K., Szaniawska, A., Caban, M., 2019. Evaluation of bioconcentration and metabolism of  
652 diclofenac in mussels *Mytilus trossulus* - laboratory study. *Mar. Pollut. Bull.* 141, 249–255.

653  
654  
655  
656  
657  
658  
659  
660  
661  
662  
663

